

Online Resource Management for the Uplink of Wideband Hybrid Beamforming System

Yuan Quan, Haseen Rahman, and Catherine Rosenberg, *Fellow, IEEE*

Department of Electrical and Computer Engineering

University of Waterloo, Canada

{yuan.quan, hrcheriy, cath}@uwaterloo.ca

Abstract—This paper studies the radio resource management (RRM) for the *uplink* (UL) of a cellular system with codebook-based *hybrid beamforming*. We consider the often neglected but highly practical multi-channel case with fewer radio frequency chains in the base station than user equipment (UEs) in the cell, assuming one RF chain per UE. As for any UL RRM, a per-time slot solution is needed as the allocation of power to subchannels by a UE can only be done once it knows which subchannels it has been allocated. The RRM in this system comprises beam selection, user selection and power allocation, three steps that are intricately coupled and we will show that the order in which they are performed does impact performance and so does the amount of coupling that we take into account. Specifically, we propose 4 online sequential solutions with different orders in which the steps are called and of different complexities, i.e., different levels of coupling between the steps. Our extensive numerical campaign for a mmWave system shows how a well-designed heuristic that takes some level of couplings between the steps can make the performance exceedingly better than a benchmark.

Index Terms—Radio resource management, Millimeter wave, Uplink, Hybrid beamforming, Massive MIMO, 5G and Beyond.

I. INTRODUCTION

Massive multi-input multi-output (MIMO) and beamforming (BF) technologies significantly enhance spectral and energy efficiency for 5G and beyond systems. Fully digital BF (FDBF) exploits the full potential of beamforming [1], but the deployment costs and power consumption are high due to the need for one RF chain per antenna. As an alternative, hybrid BF (HBF) uses far fewer RF chains than antennas by incorporating analog BF (ABF) through phase shifters, enabling support for multiple data streams on the same resource, and achieving substantial BF gain [2]. However, ABF also introduces practical constraints that must be addressed, making radio resource management (RRM) in HBF systems fundamentally different from that in FDBF systems.

Most of the work on HBF systems has been on the downlink. The uplink (UL) has received very little attention in spite of the fact that it is more and more recognized as a bottleneck in terms of perceived quality of experience [3].

We consider the UL of an OFDMA-based cellular system that uses a codebook-based HBF, i.e., the base station (BS) and the UE codebooks are given and each user is mapped to a pair of preferred beams (one at the UE and one at the BS) during beam alignment. We assume a fully connected HBF

architecture with K RF chains at the BS and one RF chain at each UE [2].

In OFDMA, the bandwidth and time resources are organized into physical resource blocks (PRBs), each one consisting of one subchannel (the bandwidth is divided in C subchannels) in a time slot. A frame is made of N_T time slots, some are reserved for the downlink (DL) and some for the UL. Each UE can send at most one stream per PRB with a maximum of K UEs allowed to transmit in total in a PRB. In the UL, the power available to each UE within a time slot is to be used in the PRBs (subchannels) allocated to that UE. This causes a coupling between user selection (USel) and power allocation (PA) that does not exist on the DL. Thus, the solutions obtained for the DL in [4] are not directly applicable to the UL. An important constraint to be taken into account is that when there is a need to select a set of beams of cardinality smaller than the number of preferred beams (recall that there is one preferred beam per user), then this beam set needs to remain the same for the entire time slot (i.e., the same set needs to be used for all PRBs in a time slot). We might not be able to select all preferred beams in all time slots because we allow $K < U$ where U is the number of UEs in the cell. In that case, per-time slot beam selection (BSel) is necessary since no more than K beams can be selected which might be smaller than the total number of beams preferred by the users (typically the number of beams at the BS is much larger than K). In this case, a UE can only be selected in a time slot if its preferred beam is selected in that time slot. Hence, per-channel solutions (e.g. [5], [6]) cannot be applied in this scenario. Of course, USel also needs to decide which subchannels to allocate to users who share the same preferred beams. Given a beam set, which users are selected in each beam in a given PRB affects the (inter-beam) interference at the BS and we will show that this cannot be ignored when performing USel.

A comprehensive study of the UL RRM of a codebook-based HBF system considering all the above steps has not been done and forms the basis of this paper. Our two research goals are: 1) to understand the impact of the inter-beam interference and of the coupling between BSel, USel, and PA on performance. 2) to propose an online efficient RRM solution for the system under consideration. Our main contributions are summarized below.

- Because of the inter-beam interference and the coupling

between BSel, USel and PA, optimizing the RRM jointly is difficult. Instead, we propose sequential online heuristics of low complexity that differ in the steps being used and in the sequence order of the different RRM steps, the order of which significantly impacts the performance.

- We first propose a *benchmark* that does not consider the coupling between RRM steps, ignores inter-beam interference, performs BSel in round-robin and uses the state-of-the-art per-beam user selection (i.e., a per-beam proportional fair uplink scheduler) as well as equal power allocation (EPA).
- Our first heuristic, S_0 , differs from the benchmark only in one step, i.e., it uses an enhanced USel algorithm, since it turns out that the state-of-the-art USel does not perform well for a small number of UEs. S_0 shows significant improvement over the benchmark.
- We then further improve the performance in S_1 by making BSel *load-aware*, i.e, by performing USel per beam, first, as in S_0 and selecting the maximum allowable beams that yield the highest individual performance metric. We keep the same USel and PA as in S_0 .
- Finally, in our ultimate heuristic, S_2 , we add a final step to S_1 to take inter-beam interference into account by revisiting USel once BSel is done.
- Our extensive numerical study on a mmWave band shows that S_2 is performing up to 6 times better than S_1 which is performing up to 91% better than S_0 which is performing up to 30% better than the benchmark (70% gain at least from S_0 to S_2), showing the importance of taking the couplings and the inter-beam interference into account as well as having a scheduler that performs well for a small number of users (since typically the number of users per beam will be small).
- Finally, we compare the performance of S_2 when we add a final step where we perform power allocation based on water-filling (WF) and show that this step is not improving the performance.

The remainder of the paper is organized as follows. Section II describes the system model. Section III provides our RRM solutions. Section IV presents our simulation results. Section V concludes the paper.

II. SYSTEM MODEL

We study the UL RRM of a single-cell massive MIMO system. The system uses a fully connected HBF architecture. Specifically, there are N_b antennas, K RF chains and $N_b \times K$ phase shifters at the BS, and N_u antennas, one RF chain and N_u phase shifters at each UE. Each RF chain is connected to all N_b (resp. N_u) antennas by N_b (resp. N_u) phase shifters at the BS (resp. UE). We assume $K \ll N_b$ and allow $U > K$ where U is the number of UEs. Assuming the system is operated in a time division duplex (TDD) mode where the full bandwidth is used for either UL or DL in a time slot.

A. The Inputs to RRM

In addition to fixed system parameters, all the online solutions rely on three input sets that are updated every time slot

or less as will be discussed next. The first set contains a pair of preferred beams for each UE (one at the BS and one at the UE). These pairs are fixed for a certain number of time slots depending on how often beam alignment (BA) is performed (see Section II-B). The second input set contains the effective channel state information (ECSI) vector ($U \times 1$) per PRB for each UE. These vectors are obtained by channel estimation (CE) using the UE's preferred beams (see Section II-C). Full CSI is not needed. Lastly, RRM steps uses per-UE weights derived from the average rate obtained in past time slots to account for proportional fairness. This will be introduced in Section II-D. Next, we introduce enough details on the BA and CE procedures to understand how the inputs are obtained.

B. Beam Alignment

We assume that ABF codebooks \mathcal{C}_b at the BS and \mathcal{C}_u at the UE have been selected in a planning phase, where $\mathcal{C}_b = \{\mathbf{w}_j \in \mathbb{C}^{N_b \times 1} : \|\mathbf{w}_j\|^2 = 1, j = 1, \dots, B_b\}$ and $\mathcal{C}_u = \{\mathbf{v}_j(u) \in \mathbb{C}^{N_u \times 1} : \|\mathbf{v}_j(u)\|^2 = 1, j = 1, \dots, B_u\}$ with B_b (resp. B_u) is the size of the codebook at the BS (resp. UE). Under the assumption that all UEs use the same codebook, we remove index u in the following. BA matches each UE with the best pair of beams, one from \mathcal{C}_b and one from \mathcal{C}_u . We call this pair, the UE's preferred pair of beams. BA can be realized by various techniques (e.g., [4], [7]). In this paper, we select the beam pair $(\mathbf{w}_u^*, \mathbf{v}_u^*)$ that provides the highest average channel gain for UE u [4]. We define $\mathcal{B}_p = \{b_1, \dots, b_{|\mathcal{B}_p|}\}$ as the set of indices of all preferred beams at the BS. We also have the mappings $b(u)$ from any UE u to the index of its preferred BS beam and $u(b)$ from any BS beam b to the UE(s) preferring BS beam b . Typically BA is done once every N_T time slots where N_T is relatively large. Our heuristics do not make any assumption on the value of N_T .

C. Effective Channel Estimation

Following BA and before RRM, each UE u transmits pilot signals using ABF vector \mathbf{v}_u^* , $1 \leq Q \leq C$ times per time slot (i.e., for each block of C/Q PRBs in a time slot). The BS measures the pilot signals of each UE and compute the effective channel coefficient in any PRB c of block q , as $g_{c,n,u}^{\text{eff}} = (\mathbf{v}_u^*)^H \mathbf{G}_{q,u}(\mathbf{w}_n^*)$ where $\mathbf{G}_{q,u}$ is the channel matrix between the BS and UE u in block q . If $n = u$, it denotes the effective signal channel between UE u and the BS. If $n \neq u$, it denotes the effective interference channel between UE n and the BS due to UE u transmission to the BS. Our heuristics do no make any assumption on the value of Q .

Note that the RRM techniques that we are about to introduce are independent of the BA and CE methods. In this paper, we posit the perfection of CE.

D. Fairness

The RRM objective is to provide proportional fairness (PF) over a certain horizon. Recall that all our solutions works on a time slot basis. Specifically, in line with what is being done in [4], [8], at the beginning of time slot i , let $R_u(i)$ be the average throughput received by u over the past W time slots.

Then, the objective in that time slot is to maximize the product of the UEs' rates over the past (and the present) $W + 1$ time slots [4], i.e.,

$$\max_{u \in \mathcal{U}} \prod (WR_u(i) + \lambda_u(i)) \approx \max_{u \in \mathcal{U}} \sum_{u \in \mathcal{U}} \frac{\lambda_u(i)}{WR_u(i)}, \quad (1)$$

where $\lambda_u(i)$ is the rate of UE u in time slot i which is the sum of the rates seen in each PRB of that time slot. This can be approximated by a weighted sum rate maximization where the weight of user u is $w_u(i) = 1/R_u(i)$ as long as $WR_u(i) \gg \lambda_u(i)$, which is reasonable to assume. At the end of time slot i , we use a moving average of size W to update $R_u(i)$ as $R_u(i+1) = (1 - 1/W)R_u(i) + \lambda_u(i)/W, \forall u \in \mathcal{U}$ and the weight becomes $w_u(i+1) = 1/R_u(i+1)$. For brevity of notation, we will remove the time slot index i .

Finally, note that the natural performance metric for PF is the geometric mean of the rates GM , as discussed in [4], i.e., given a time horizon of N_T time slots,

$$GM = \left(\prod_{u=1}^U \frac{1}{N_T} \sum_{i=1}^{N_T} \lambda_u(i) \right)^{\frac{1}{U}}. \quad (2)$$

E. Rate Function

Given a selected beam set and given that user set z has been selected in a given PRB c , the signal-to-interference-plus-noise ratio (SINR) of UE $u \in z$ is

$$\gamma^{c,u}(z) = \frac{|g_{c,u,u}^{\text{eff}}|^2 p^{c,u}(z)}{\sum_{\substack{n \in z \\ n \neq u}} |g_{c,u,n}^{\text{eff}}|^2 p^{c,n}(z) + \sigma_{\text{PRB}}^2}, \quad (3)$$

where σ_{PRB}^2 is the noise power on a PRB and $p^{c,u}(z)$ is the power allocated to PRB c by UE u . Hence, to obtain the SINRs, we need to do power allocation, i.e., distribute the UE's power budget to its allocated PRBs.

We use a rate function based on practical modulation and coding schemes (MCSs) rather than Shannon capacity formula to map the SINR of a UE in a given PRB to the maximum achievable data rate in bps in this PRB. Specifically, we model the rate function as a piecewise constant function of SINR, consisting of L levels corresponding to the L MCSs, i.e.,

$$f(\gamma) = B_c (s_1 \mathbb{1}_{[\Gamma_1, \Gamma_2)}(\gamma) + \dots + s_L \mathbb{1}_{[\Gamma_L, \infty)}(\gamma)), \quad (4)$$

where B_c is the bandwidth of a PRB in Hz, $\mathbb{1}_A(x)$ is the indicator function, which equals 1 if $x \in A$ and zero otherwise, Γ_l denotes the SINR decoding threshold for MCS l and s_l is the spectral efficiency of MCS l measured in bps/Hz. The set of MCSs is adopted from 3GPP TS 38.214 [9].

III. RADIO RESOURCE MANAGEMENT

In this section, we present our four online solutions (including the benchmark). Our goal is to identify what are the aspects of the various RRM steps that have a significant impact on the performance of the system. Recall that the UL RRM includes the following steps:

- 1) *Beam selection (BSel)*: Let $L = \min(|\mathcal{B}_p|, K)$, representing the maximum number of beams we can select. In each

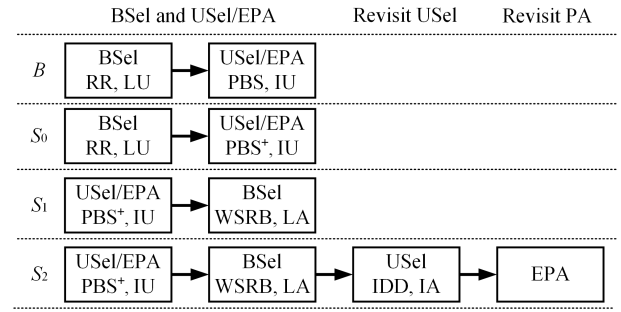


Figure 1: Our RRM solutions: RR: round robin, IU: interference unaware, IA: interference aware LA: load aware, LU: load unaware, EPA: equal power allocation, PBS: per beam selection, WSRB: weighted sum rate beam selection.

time slot, up to L beams are selected for transmission. The selected beams are fixed for all subchannels in a time slot. Recall that beams may have different “loads” (a term we use loosely) because the numbers of UEs preferring each beam are different.

- 2) *User selection (USel)*: Within a time slot, for each beam of the selected subset of beams, at most one UE is to be selected in each subchannel. This is coupled with beam selection because a UE can only be selected if its preferred BS beam is activated in the time slot. Note that there might be significant inter-beam interference at the BS since multiple (up to L) UEs can transmit on the same subchannel.

- 3) *Power allocation (PA)*: The power budget of each UE needs to be allocated to the subchannels on which it is selected for transmission. Hence, PA is clearly coupled with USel.

Next, we propose four sequential online heuristics (one of them being the benchmark) of low complexity that differ in the steps being used and in the sequence order of the different RRM steps, the order of which significantly impacts the performance. Fig. 1 shows the sequence of steps of all four solutions and the main attributes of the steps.

A. RRM Benchmark

We first build a basic RRM solution as the benchmark (called B in the following). Given a time slot:

- For BSel, we select a beam set of size L from \mathcal{B}_p in a round-robin (RR) fashion (one beam set per time slot). This BSel is load-unaware (LA), i.e., it does take into account the fact that some beams might be preferred more than others.
- For USel and equal power allocation (EPA) jointly: Given the selected beam set in a time slot, we select one UE per PRB for each beam independently without considering the inter-beam interference, hence USel is interference-unaware (IU). Specifically, for each subchannel within a time slot, we select at most one UE from those preferring the given beam ($u(b)$), assuming that this beam is the only active one in that time slot. Focusing on one beam, this is similar to single-user (SU) MIMO user scheduling.

Hence, the solution in [10], called per beam selection (PBS), can be applied to generate the per-beam user selection results. PBS selects UEs in a greedy way taking their weights into account. In each step, it first assumes each UE is given one more subchannel among those not yet allocated (its highest gain subchannel), and calculates a revised weighted rate for each UE in the time slot assuming EPA. Under this assumption, PBS finds the UE whose weighted rate increases the most and gives its preferred subchannel. The algorithm stops if there are no more subchannels to give or if none of the UEs see an increase in rate.

Note that PBS gives us not only a user set per subchannel but also a power allocation (based on EPA). Hence, we have everything we need to compute the SINRs in this time slot, the rates and update the weights.

B. S_0 : Improving on PBS

Extensive simulation campaigns have shown that PBS does not perform well when the number of users preferring a beam is small (which is often the case in practice, e.g, if you have a cell with 40 users and 32 beams, there are just a few users preferring a specific beam). In that case, we found out that PBS might stop allocating subchannels to users too early, and that even if adding a subchannel might not increase the rate seen by a user, adding more than one might do it. We implement a persistent search strategy in which we do not stop allocating subchannels to a UE as soon as we see a decrease in its rate. This strategy can improve the performance by up to 27% based on our results. Specifically, We propose an enhanced version of PBS, PBS^+ , in which the search, for a UE, is stopped once we see X cumulative iterations with a decrease in rate. We describe PBS^+ in Alg. 1 for a given selected beam b and a given time slot. PBS^+ can be run independently for all selected beams because a UE selects one preferred BS beam. Note that the inputs to the algorithm are the set $u(b)$ of users preferring beam b , X , the weights w_u , per user power P_{UE} and the set of all the effective channel gains $\mathcal{G}_{eff}^b = \{g_{c,n,u}^{eff}, \forall n, u \in u(b)\}$ and for all subchannels c .

S_0 has the same sequence of steps as the benchmark. The only difference is that we use PBS^+ instead of PBS as the joint per beam USel and PA.

C. S_1 : Load-Aware Beam Selection

In the previous two solutions, we select beams first in a RR fashion without considering the loads (i.e., the numbers of UEs preferring a beam) of a beam which affects the overall fairness. In the third solution S_1 , we restructure the RRM sequence by moving USel before BSel. This approach allows for an estimation of load before performing BSel, enabling load-aware BSel. Note that if $|B_p| < K$, all preferred beams can be selected and there is no difference between S_0 and S_1 .

Specifically, at the beginning of a time slot, we first run PBS^+ independently on each beam in B_p . Then we compute the per-beam weighted sum rate and select the L beams with

Algorithm 1 PBS^+ on beam b , Inputs: $u(b)$, X , w_u , P_{UE} , \mathcal{G}_{eff}^b

- 1: Set the stop flags and the sum-rate $SR(u)$ of all UEs in beam b to zero.
 - 2: **while** there are any remaining subchannels to allocate in this time slot **and** UEs whose stop flag is no larger than X **do**
 - 3: **for** each UE in this beam whose stop flag is no larger than X **do**
 - 4: Select the best remaining channel ($\max_c g_{c,u,u}^{eff}$) for this UE.
 - 5: Calculate $SR(u)$ of this UE in this time slot assuming EPA and that this channel is allocated to it.
 - 6: Increase its stop flag by one if the sum rate of this UE does not increase.
 - 7: **end for**
 - 8: Select the UE whose weighted sum rate increases the most and allocate its best remaining channel to it.
 - 9: Update the sum-rate $SR(u)$ of that UE.
 - 10: **end while**
-

the highest weighted sum rates. This LA BSel method is referred to as weighted sum rate BSel (WSRB).

D. S_2 : Interference-Aware Two-Step USel

In the previous three solutions, the per-beam user selection does not consider the inter-beam interference in a subchannel. Hence interference is ignored in the whole RRM process, making the approach interference-unaware (IU). Nevertheless, inter-beam interference can significantly affect the rate achieved by each UE when multiple UEs share the same subchannel. To address this, we propose an interference-aware USel approach that is done in two steps. Specifically, referring to S_1 , we add a step, called interference down dropping (IDD), after BSel to revisit USel, i.e., to possibly deselect UEs in a subchannel if they generate large interference at the base station (e.g, a level I_D times larger than the signal strength of any other UE within the subchannel).

To explain IDD in more detail, we need some notations. Note that IDD is done independently per subchannel. Given a subchannel c , let $I_{c,n,u} = \frac{|g_{c,n,u}^{eff}|^2 p^{c,u}}{|g_{c,n,n}^{eff}|^2 p^{c,n}}$ be the ratio between the interference impacting the transmission between UE n and the BS due to the transmission of UE u to the BS and the signal power of UE n at the BS. It is set as zero if $n = u$. We further define $\mathcal{I}_{c,u} = [I_{c,n_1,u}, \dots, I_{c,n,u}, \dots, I_{c,n_{|z_c|},u}]^T$ for $\forall n \in z_c$.

The details of IDD are described in Alg. 2 for subchannel c . The inputs are the user set z_c obtained after the first two steps in S_1 , I_D as well as $\mathcal{I}_{c,u} \forall u \in z_c$.

This algorithm deselects UEs potentially causing too much interference to other UEs at the BS. We refer to this process as IDD. Once, IDD has been applied to all subchannels, we redo EPA. In Section IV, we will compare the performance with and without this process to understand its significance.

Algorithm 2 *Interference Down Dropping for subchannel c*
Inputs: $\{\mathcal{I}_{c,u}, \forall u \in \mathcal{U}\}$, I_D

- 1: **for** each $u \in \mathcal{U}$ **do**
- 2: Verify if any element in $\mathcal{I}_{c,u}$ is larger than I_D .
- 3: If yes, record the UE.
- 4: **end for**
- 5: Deselect the recorded UE(s) in this subchannel.

E. Ultimate water filling (WF)-based Power Allocation

We can add an extra step at the end of S_2 , in which we apply water filling (WF)-based PA [11] to allocate the power of each UE to the subchannels they occupy in a time slot. This step adds complexity but may be necessary to improve performance. We will compare the performance with and without this extra step in Section IV for S_2 .

IV. NUMERICAL RESULTS

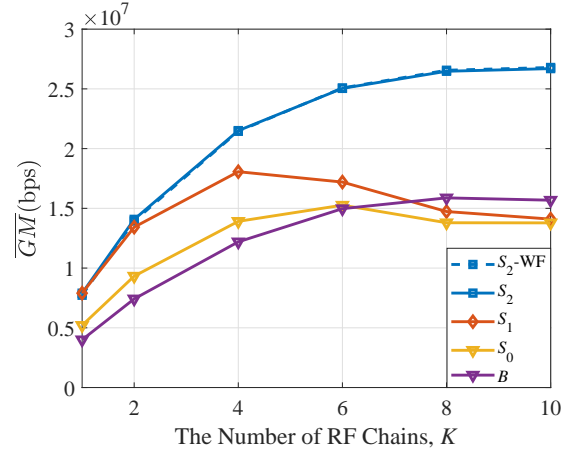
In this section, we present the numerical results for our four solutions, namely the benchmark, S_0 , S_1 and S_2 in a mmWave single cell. Specifically, we consider the uplink of a small cell with a radius of $r = 75$ m, with UEs uniformly distributed excluding a 6 m radius around the BS where path loss models are invalid. The BS height is 10 m. Each UE has a power budget of $P_{UE} = 7$ dBm and the noise power spectral density N_0 is -174 dBm/Hz. The BS and UEs use uniform linear antenna arrays (ULAs) with 128 and 16 antennas, respectively, spaced in half-wavelength. The system operates at 28 GHz with a 100 MHz bandwidth, divided into $C = 132$ subchannels of $B_c = 720$ kHz. We assume $Q = 22$, i.e., a coherence bandwidth of 4.32 MHz which is typical in a mmWave small cell [4]. We set the horizon to be $N_T = 100$ time slots. We generate ABF codebooks for the BS and UEs using the method in [12].

We adopt a wideband channel model which incorporates multipath effects, i.e., scattering clusters and spatial paths in each cluster [4]. The MIMO channel between BS and UE u at block q is defined as the following $N_u \times N_b$ matrix:

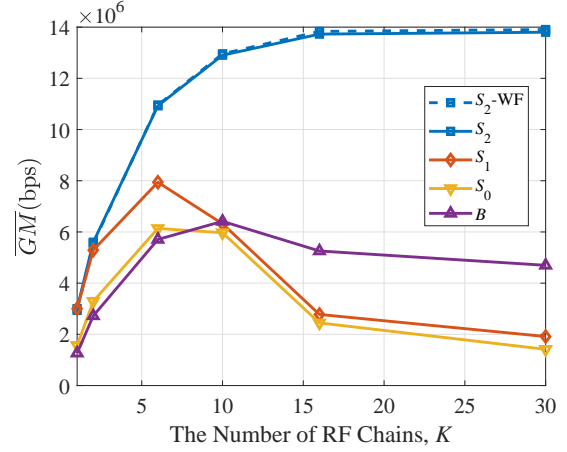
$$\mathbf{G}_{q,u} = \frac{1}{\sqrt{N_{\text{path}}}} \sum_{d=1}^{N_{\text{cluster}}} \sum_{l=1}^{N_{\text{path}}} g_{d,l}^u e^{-j2\pi\tau_{d,l}^u f_q} \mathbf{a}_{\text{RX}}(\phi_{d,l}^u) \mathbf{a}_{\text{TX}}^H(\theta_{d,l}^u), \quad (5)$$

where N_{cluster} is the number of clusters, N_{path} is the number of paths in each cluster, $g_{d,l}^u$ is the coefficient of the path l of cluster d , f_q is the center frequency of block q , and $\tau_{d,l}^u = \tau_{0,d}^u + \tau_{1,d,l}^u$ in which $\tau_{0,d}^u$ is the group delay of the d -th cluster and $\tau_{1,d,l}^u$ is the relative path delay of the l -th path in the d -th cluster. Moreover, $\theta_{d,l}^u$ and $\phi_{d,l}^u$ represent the AoD and the AoA corresponding to the l -th path of cluster d of the channel. We assume the large-scale fading, AoAs and AoDs remain fixed for the N_T time slots. Additionally, $\mathbf{a}_{\text{TX}}(\cdot)$ and $\mathbf{a}_{\text{RX}}(\cdot)$ are the array response vectors at the BS and UE u . We generate the specified parameters and functions as in [4, Section IV-F].

We define a realization as U uniformly distributed UEs with the corresponding Q channel parameters per UE for each of $N_T = 100$ time slots. The performance is the GM of the UEs'



(a) $U = 10$

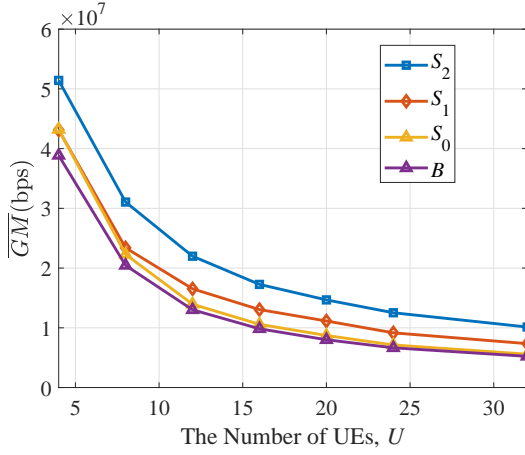


(b) $U = 30$

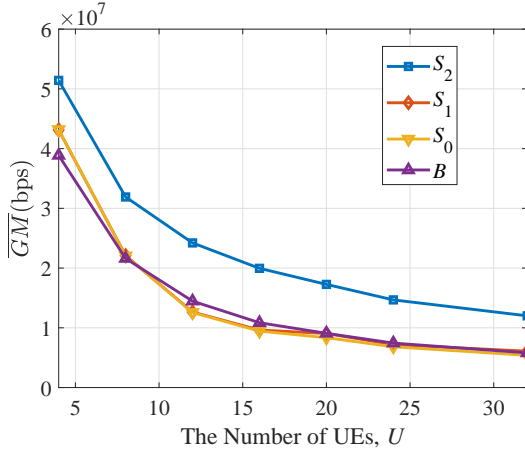
Figure 2: \overline{GM} vs. K with fixed U , $N_b = 128$, $N_u = 16$, $B_b = 32$, $B_u = 4$.

rates over the $N_T = 100$ time slots. In each realization, we perform BA, once at the beginning, and run the RRM solution for N_T consecutive time slots. We set the initial W as 10 and R_u as 2 in the first time slot. After testing multiple values, we found that $X = 6 = \frac{C}{Q}$ and an update step length of X channels instead of one in Alg. 1 and $I_D = 1$ in Alg. 2 can provide good performance and efficiency. Next, we provide the numerical results. \overline{GM} is the GM averaged over 50 different realizations in Fig 2 and 200 different realizations in Fig 3.

We first compare the performance of B , S_0 , S_1 and S_2 for $U = 10$ in Fig. 2a and $U = 30$ in Fig. 2b where we plot \overline{GM} as a function of K , the number of RF chains. We also show the performance of S_2 when we add the extra step with WF PA (the curve is labeled S_2 -WF). PBS^+ (see S_0 versus B) increases the performance by 30% when $K = 1$ and $U = 10$. Note that PBS^+ does not do well when either K is large or U is large because PBS^+ schedules more users than PBS , creating more interference and neither B nor S_0 are IA. The LA BSEL, WSRB, (see S_1 versus S_0) improves the performance by 91% wrt S_0 with $U = 30$ and $K = 1$ and by 29% for $U = 30$ and $K = 6$. Note that S_0 and S_1 tend to select



(a) $K = 6$



(b) $K = 10$

Figure 3: \overline{GM} vs U with fixed K , $N_b = 128$, $N_u = 16$, $B_b = 32$, $B_u = 4$.

more UEs than B , which increases interference and this leads to a notable performance drop when K is large. However, this side-effect is mitigated by the IA user dropping scheme (IDD), resulting in a non-decrease in performance when K increases and an outstanding performance increase of 621% (S_2 versus S_1) for $U = 30$ and $K = 30$. Clearly S_2 is more useful when the number of users is larger.

Figs. 2 also show that there is no need to add an extra WF PA step to S_2 since it does not impact performance. Finally, we note that the performance of S_2 reaches a plateau when K increases and that $K = 6$ RF chains (resp. $K = 10$) can achieve at least 90% of the plateau when $U = 10$ (resp. $U = 30$) in S_2 . Next, we show the performance of our four solutions as a function of U , the number of UEs for two values of K , i.e., $K = 6$ in Fig. 3a and $K = 10$ in Fig. 3b. In both figures, S_2 outperforms all the other solutions by roughly 38% for $K = 6$ and 97% for $K = 10$. Therefore, neglecting interference limits the full potential of well-designed BSEL and USEL.

Finally, we analyze the complexity of each step in our four heuristics in Table I, assuming we process in parallel PBS⁺ for all the beams for S_1 and S_2 and PBS (resp. PBS⁺) for B

Table I: Complexity of the four solutions

	USEL	BSEL	IDD	Overall
B	$\mathcal{O}(CU)$	$\mathcal{O}(L)$	\times	$\mathcal{O}(CU)$
S_0	$\mathcal{O}(CU)$	$\mathcal{O}(L)$	\times	$\mathcal{O}(CU)$
S_1	$\mathcal{O}(CU)$	$\mathcal{O}(\mathcal{B}_p)$	\times	$\mathcal{O}(CU)$
S_2	$\mathcal{O}(CU)$	$\mathcal{O}(\mathcal{B}_p)$	$\mathcal{O}(U)$	$\mathcal{O}(CU)$

(resp. S_0) for the L beams. We also assume that we process in parallel Alg. 2 for all the subchannels in a time slot. The main complexity is the USEL since it adds channels to UEs in an iterative manner. WSRB BSEL and IDD have negligible complexity because $|\mathcal{B}_p| < U \ll CU$. The overall complexity of all the four schemes are the same which confirms that S_2 is suitable for real-time operation.

V. CONCLUSION

We have investigated the uplink radio resource management in a codebook-based HBF system considering multiple channels per time slot and a limited number of RF chains ($K < U$). We have shown that beam selection, user selection and power allocation are intricately coupled and that the sequence in which these steps are executed, to take part of the coupling(s) into account, significantly impacts the proportional fairness performance of the system. In particular, load-aware (LA) beam selection and interference-aware (IA) user selection have a huge impact on performance as shown by our extensive numerical campaign for a mmWave single cell. Our LA and IA solution, S_2 performs six times better than the best of the other considered solutions and has a reasonable complexity.

REFERENCES

- [1] T. L. Marzetta and H. Yang, *Fundamentals of massive MIMO*. Cambridge University Press, 2016.
- [2] A. F. Molisch, V. V. Ratnam, S. Han, Z. Li, S. L. H. Nguyen, L. Li, and K. Haneda, "Hybrid beamforming for massive MIMO: A survey," *IEEE Communications Magazine*, vol. 55, no. 9, 2017.
- [3] E. C. Strinati and S. Barbarossa, "6G networks: Beyond Shannon Towards Semantic and Goal-Oriented Communications," *Computer Networks*, vol. 190, p. 107930, 2021.
- [4] Y. Quan, S. Shahsavari, and C. Rosenberg, "Planning and operation of millimeter-wave downlink systems with hybrid beamforming," *IEEE Transactions on Wireless Communications*, pp. 1–1, 2024.
- [5] H. Li, T. Q. Wang, X. Huang, J. A. Zhang, and Y. J. Guo, "Low-complexity multiuser receiver for massive hybrid array mmwave communications," *IEEE Trans. on Communications*, vol. 67, no. 5, 2019.
- [6] Z. Wang, M. Li, R. Liu, and Q. Liu, "Joint user association and hybrid beamforming designs for cell-free mmwave mimo communications," *IEEE Trans. on Communications*, vol. 70, no. 11, 2022.
- [7] N. Barati, A. Hosseini, M. Mezzavilla, T. Korakis, S. Panwar, S. Rangan, and M. Zorzi, "Initial access in millimeter wave cellular systems," *IEEE Trans. on Wireless Communications*, vol. 15, no. 12, 2016.
- [8] Y. Özcan, J. Oueis, C. Rosenberg, R. Stanica, and F. Valois, "Robust planning and operation of multi-cell homogeneous and heterogeneous networks," *IEEE Transactions on Network and Service Management*, vol. 17, no. 3, 2020.
- [9] 3GPP, "NR; Physical layer procedures for data," *3rd Generation Partnership Project (3GPP), Technical Report (TR) 38.214*, 2022.
- [10] J. Huang, V. Subramanian, R. Agrawal, and R. Berry, "Joint scheduling and resource allocation in uplink ofdm systems for broadband wireless access networks," *IEEE JSAC*, vol. 27, no. 2, 2009.
- [11] C. Xing, Y. Jing, S. Wang, S. Ma, and H. V. Poor, "New viewpoint and algorithms for water-filling solutions in wireless communications," *IEEE Transactions on Signal Processing*, vol. 68, 2020.
- [12] J. Song, J. Choi, and D. Love, "Codebook design for hybrid beamforming in millimeter wave systems," in *IEEE ICC*, 2015.